Application of optical measurement techniques for experimental modal analyses of lightweight structures

C. Schedlinski[1], J. Schell[2], E. Biegler[2], J. Sauer[2]

[1] ICS Engineering GmbH
Am Lachengraben 5, 63303 Dreieich, Germany
e-mail: **sched@ics-engineering.com**

[2] Polytec GmbH
Polytec-Platz 1-7, 76337 Waldbronn, Germany

Abstract

In this paper, different excitation methods for experimental modal analysis are assessed by example of a lightweight aluminum cover in conjunction with classical acceleration measurements and laser scanning vibrometry. It will particularly be shown that one of the greatest advantages of laser scanning vibrometry, namely the massless and practically interaction free automated response measurement of lightweight structures can be compromised significantly if shaker excitation is employed. Since these effects usually cannot be fully quantified and eliminated in the following they may especially jeopardize the successful outcome of subsequent model validation campaigns.

1 Introduction

State of the art optical measurement techniques like laser scanning vibrometry (LSV) are most suited when lightweight structures are to be investigated especially if a high spatial measurement resolution of the test piece is demanded for. The lack of physical sensors with discrete mass fully removes the problem of massloading the structure during the test and therefore eliminates the risk of adverse varying frequency shifts which may occur when classical roving sensor measurement methods are employed.

Due to the typically high spatial measurement resolution during LSV measurements manual excitation is prohibitive and thus the test must be automated. Here, shaker excitation is usually the method of choice. However, the required force measurement (sensor) and the coupling of the shaker to the structure (push-rod/stinger) can as well inflict significant perturbations on the system (additional mass of sensor, potential additional forces and moments due to stinger system, damping effects due to micro friction between structure and force sensor).

In the following, an alternative option using automated hammer excitation is presented that eliminates practically all negative effects due to interaction of sensors with the lightweight structure to be tested. In detail, the excitation is applied using a special hammer device (see [1]) that allows for a highly reproducible, fully automated hammer test capable of supporting LSV tests with very large numbers of measurement points.

The approach is compared to LSV measurements with shaker excitation as well as to classical acceleration measurements in order to directly evaluate the quality of the results and to assess the advantages and disadvantages of both excitation options. Furthermore, it will be shown that the effects of the shaker connection and the force sensor – in case of the investigated structure – perturb the experimental modal data such that they cannot be fully compensated anymore. Also subsequent application of model validation techniques is not able to mitigate the effects and thus erroneous validation results will be obtained.

2 Test item and conducted tests

In Figure 1 the tested lightweight aluminum cover is shown. The mass of the cover is 860g and the dimensions are about 305x165x33 mm.

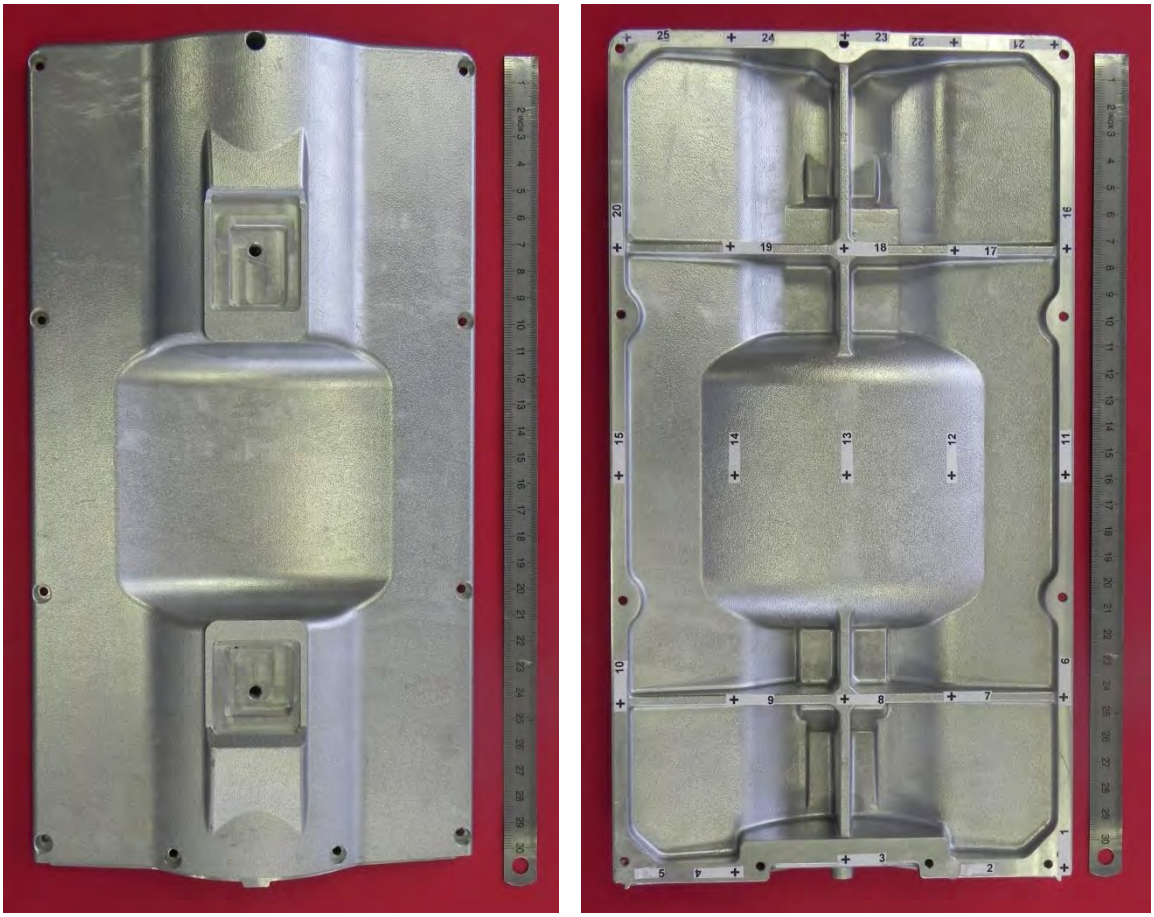

Figure 1: Test item top (left), bottom (right) with measurement points for classical acceleration measurements

In order to assess the advantages and disadvantages of the different excitation methods the following tests were conducted:

- Acceleration measurements (Reference/classical test)
  - hammer excitation (manual)
    - roving hammer modal test
    - two fixed lightweight miniature accelerometers (0.2 g) as reference sensors
    - minimized mass loading
- LSV measurements (fully automated – no manual interaction required)
  - hammer excitation (automated)
    - roving laser modal test (automated scanning) – no mass loading
  - shaker excitation
    - roving laser modal test (automated scanning) – mass loading by impedance head

The cover was tested suspended in bungee cords under quasi free/free boundary conditions. Figure 2 shows the setup for the classical hammer test; Figure 3 the laser test with automated hammer and shaker excitation.

Figure 2: Survey of classical hammer test (reference test)

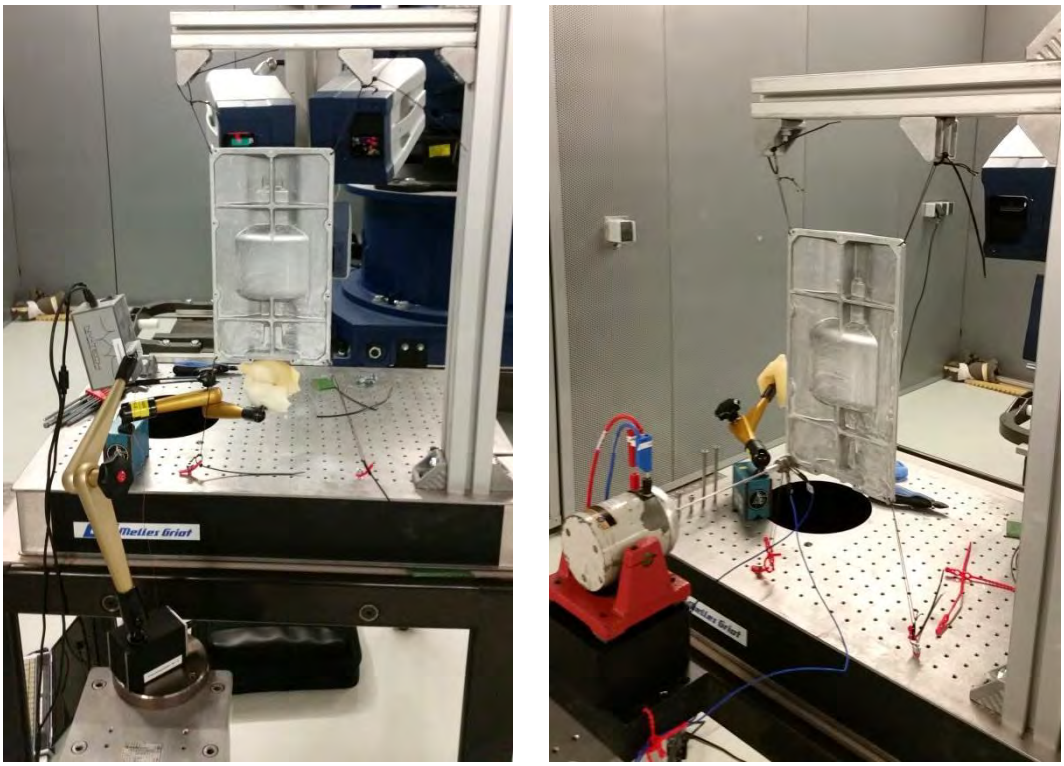

Figure 3: Survey of LSV test with automated hammer (left) and automated shaker excitation (right)

The test parameters for the three conducted tests are summarized in Table 1 and the corresponding test models are shown in Figures 4 and 5. For the LSV test models according to Figure 5 only the measured test nodes are shown. For the LSV hammer test slightly less measurement points could be measured due to increased movement of the cover as a result of the hammer impacts.

Description	**Hammer/Ref. Value**	**Hammer/LSV Value**	**Shaker/LSV Value**
Frequency Range	0…6,400 Hz	0.98…10,000 Hz	40…6,400 Hz
Frequency Resolution	0.25 Hz	0.98 Hz	1 Hz
Spectral Lines	25,601	10,240	6,361
Frames per Average	7	4	8
Windows Applied	Exponential	Exponential	None
Measurement Type	Roving Hammer	Roving Laser	Roving Laser
Excitation Type	Hammer (Manual)	Hammer (Automatic)	Shaker (Pseudo Random)
Number of Test Nodes	25	6,591	7,212
Reference Locations	2	1	1

Table 1: Summary of test setups

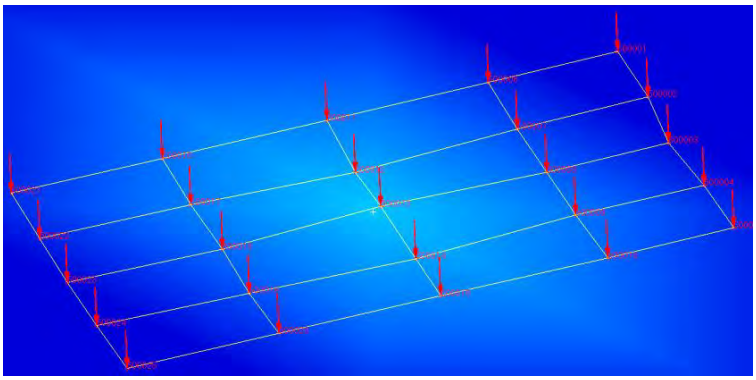

Figure 4: Test model for reference hammer test (with measured directions)

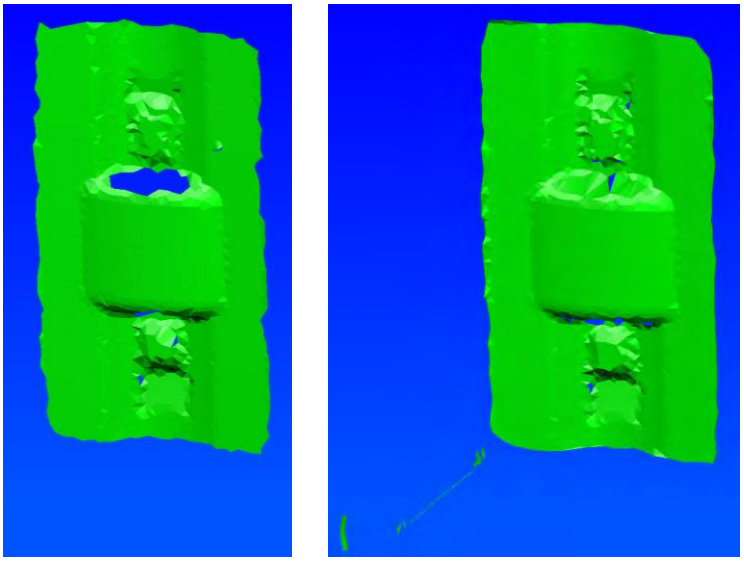

Figure 5: Test model for LSV hammer test (left) and LSV shaker test (right)

3 Test results

The following figures exemplarily show selected measured frequency response functions (FRFs) of the reference measured during all three tests. In detail all corresponding FRFs are shown for the reference hammer test in Figure 6. Figure 7 shows a comparison of the reference FRF for the three tests. It can be noticed that the cover exhibits very low damping and clear and pronounced peaks are to be observed.

From Figure 7 it can be seen that some differences exist between the three conducted tests. For the two hammer tests only damping differences can be observed. These can be contributed to foam material used during the LSV hammer test to limit the movements of the plate due to the hammer impacts during the test (see also figure 3, left) that led to increased damping. For the shaker test, however, not only increased damping can be observed. In addition peak shifts and additional resonances are found.

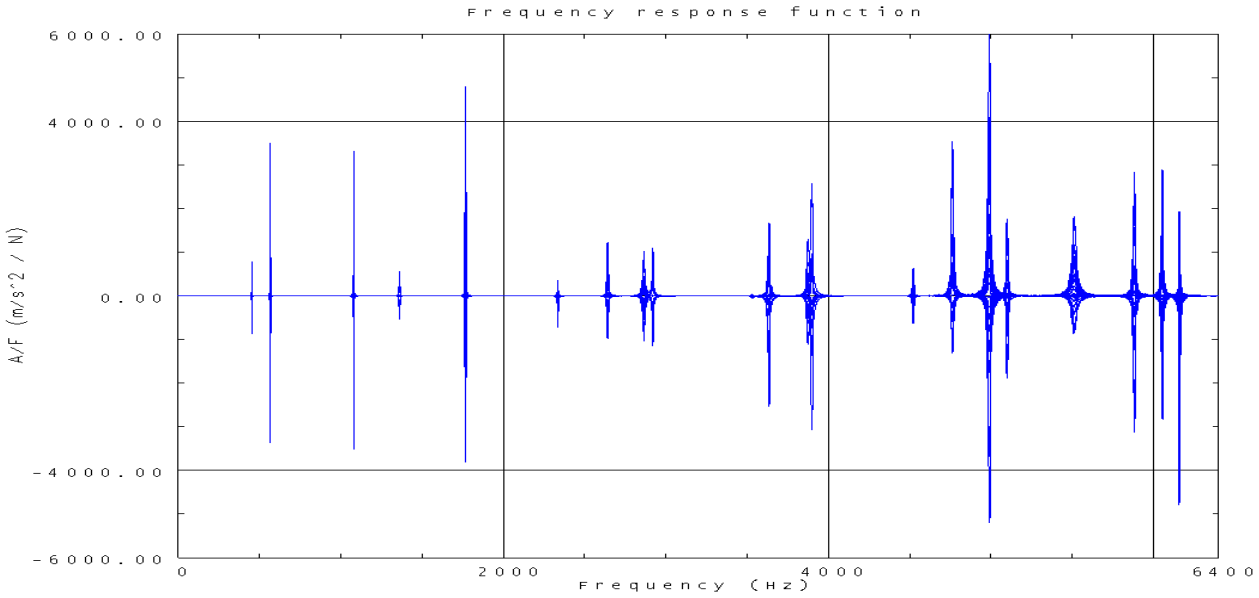

Figure 6: All measured frequency response functions, Hammer/Reference

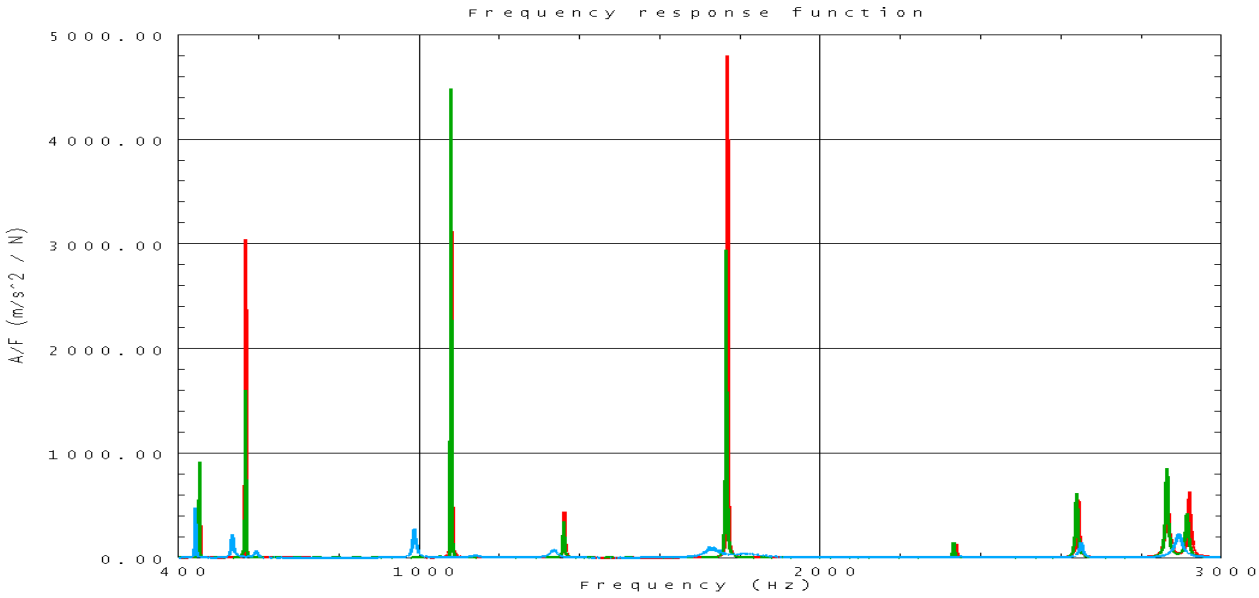

Figure 7: Comparison of reference FRF of all three tests (detail up to 3 kHz)
Hammer/Reference (red), Hammer/LSV (green), Shaker/LSV (blue)

The experimental modal analysis provided nine mode shapes for the hammer tests and 13 for the shaker test up to about 3 kHz according to Table 2. Figure 8 shows the Auto-MAC matrices of the identified mode shapes; Figures 9 and 10 exemplarily show the first mode at about 450 Hz and the ninth mode at about 3 kHz for the three tests. It can nicely be seen that the LSV measurements provide a much better visual representation of the modes especially in the higher frequency range due to the high spatial resolution of the measured points.

For the hammer tests it can be noted that they provide the same number of modes and the corresponding Auto-MAC matrices are very well decoupled. Also the observed frequency deviations between the two tests are rather low. Therefore it can be expected that comparable results have been obtained.

For the LSV shaker test, however, larger frequency deviations are found and additional modes can be identified. This can be contributed to additional local bending modes of the stinger that couple into the system. The explanation for this is that the force measured by the impedance head only decouples the axial motion of the stinger from the plate. Now, eventual bending modes of the stinger that fall into the observed frequency range (see also Figures 9 and 10, right) introduce additional moments to the system that are not measured. Thus the bending related properties of the stinger also become part of the measured system.

No.	Hammer/Ref. Frequency [Hz]	Hammer/LSV Frequency [Hz]	No.	Shaker/LSV Frequency [Hz]	Description
1	453.78	452.15	1	442.20	1st bending
2	568.42	567.26	2	534.72	1st torsion
-	-	-	3	596.28	stinger (1st bending)
-	-	-	4	621.00	ditto
3	1081.34	1079.79	5	989.08	2nd torsion
-	-	-	6	1142.38	stinger (2nd bending)
4	1363.49	1360.72	7	1336.76	2nd bending
5	1769.39	1766.14	8	1726.91	3rd torsion
-	-	-	9	1822.47	stinger (3rd bending)
6	2337.71	2332.96	10	2352.24	1st bending about short edge
7	2644.03	2639.55	11	2651.21	ditto front/rear out of phase
8	2867.14	2864.66	12	2893.87	ditto, mid out of phase
9	2921.17	2914.78	13	3031.78	4th torsion

[1)] Mode Shapes normalized to maximal value one

Table 2: Experimental modal analysis results

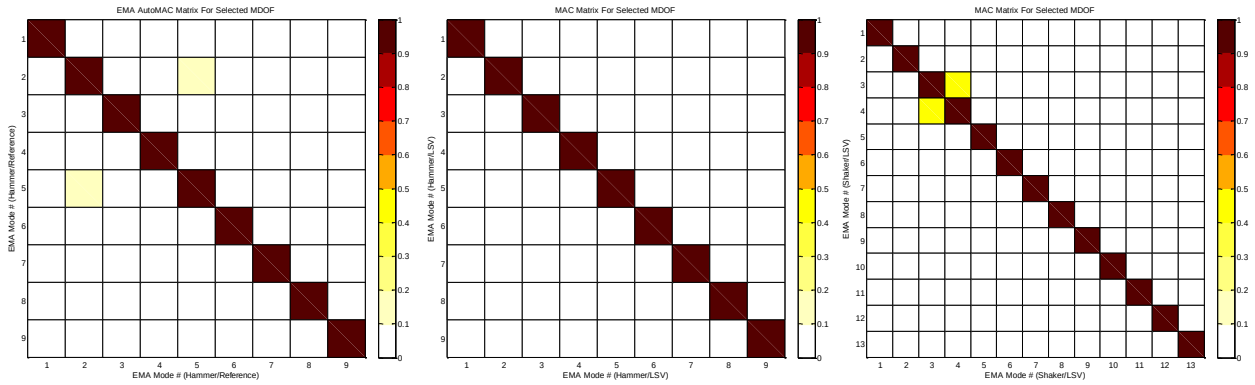

Figure 8: Test mode shape Auto-MAC matrices for
Hammer/Reference (left), Hammer/LSV (mid), Shaker/LSV (right)

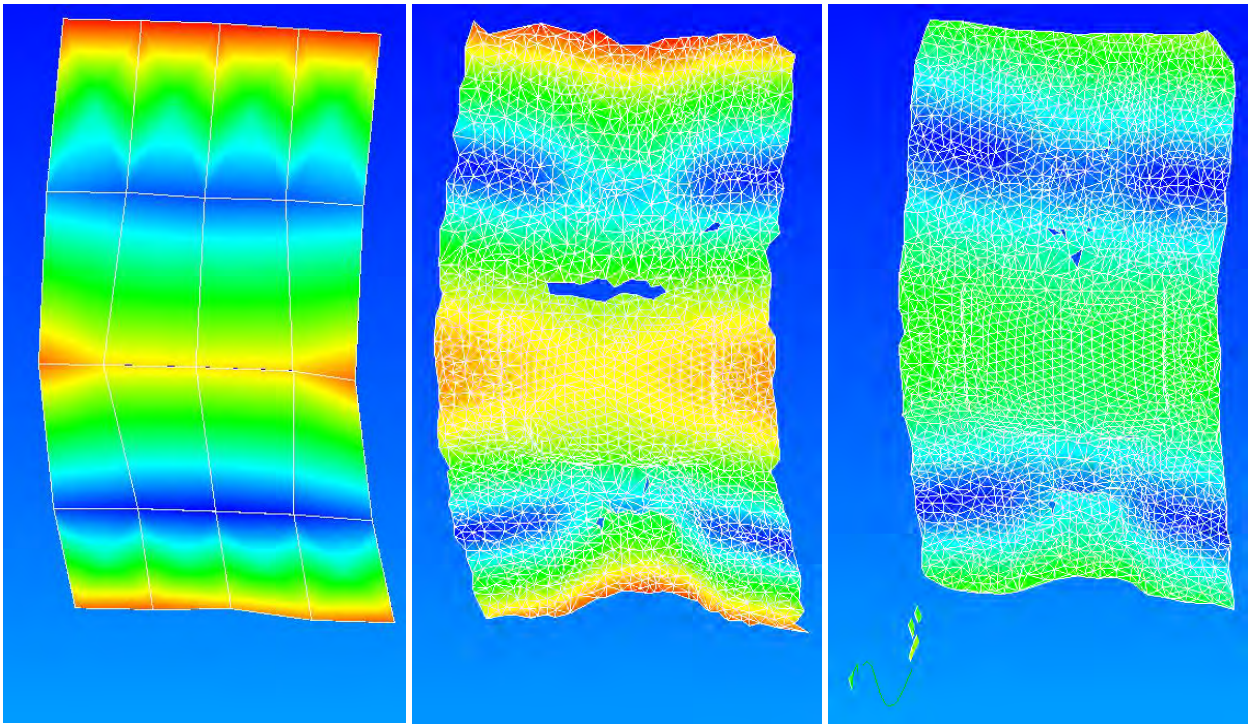

Figure 9: Mode 1 at about 450 Hz for Hammer/Ref. (left), Hammer/LSV (mid), and Shaker/LSV (right)

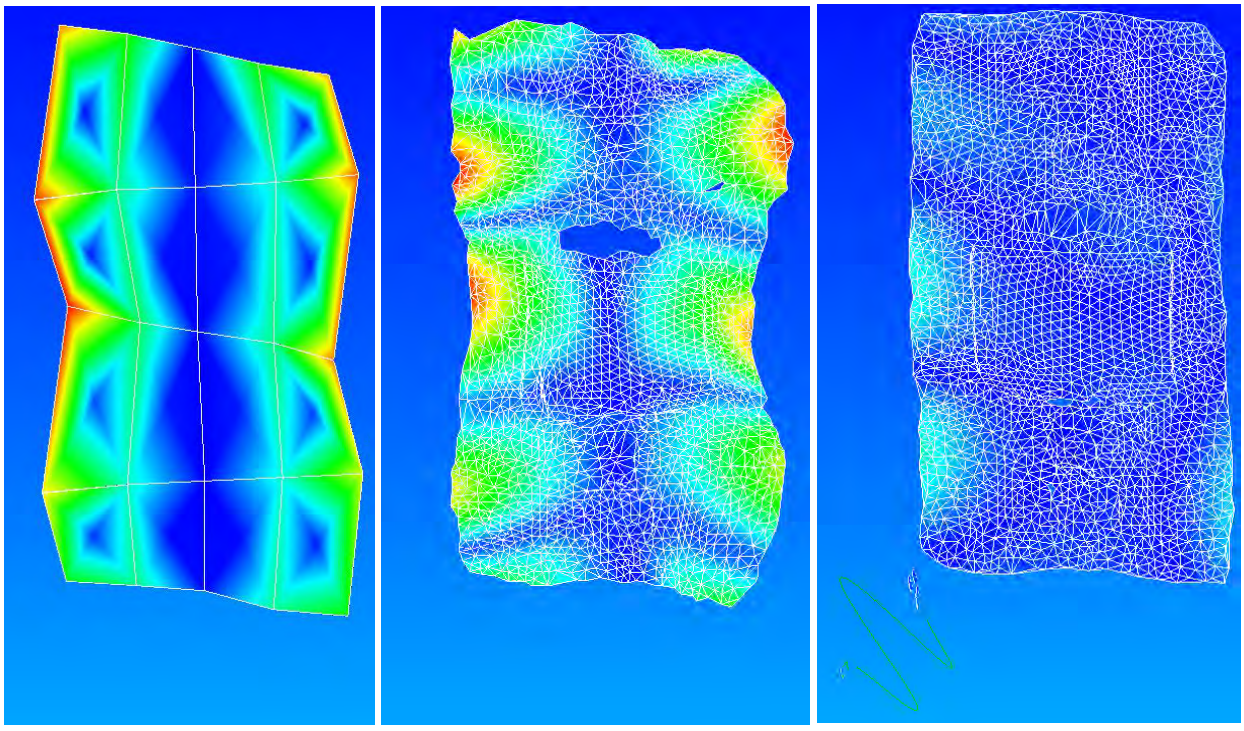

Figure 10: Mode 9 at about 3 kHz for Hammer/Ref. (left), Hammer/LSV (mid), and Shaker/LSV (right)

4 Test/test and test/analysis correlation

Table 3 and Figure 11 show a comparison of the reference hammer test with the LSV hammer test and LSV shaker test respectively. The results of the hammer test correspond very well with frequency deviations smaller than 0.4% and MAC values greater than 95%. For the LSV shaker test the results differ

noticeably, as already observed above, with frequency deviations from about -9% to 6% and MAC values as low as 60%. The selected impedance head/stinger assembly thus considerably alters the system leading to significant systematic errors.

No.	Ref. Ham. [Hz]	LSV Ham. [Hz]	Dev. [%]	MAC [%]	LSV Shak. [Hz]	Dev. [%]	MAC [%]
1	453.78	452.15	-0.36	99.58	442.20	-2.55	98.73
2	568.42	567.26	-0.20	99.42	534.72	-5.93	96.89
3	1081.34	1079.79	-0.14	99.14	989.08	-8.53	91.84
4	1363.49	1360.72	-0.20	99.06	1336.76	-1.96	86.08
5	1769.39	1766.14	-0.18	98.86	1726.91	-2.40	95.61
6	2337.71	2332.96	-0.20	98.11	2352.24	0.62	97.12
7	2644.03	2639.55	-0.17	95.67	2651.21	0.27	91.86
8	2867.14	2864.66	-0.09	98.27	3031.78	5.74	61.38
9	2921.17	2914.78	-0.22	98.10	2893.87	-0.93	79.16

Table 3: Test/test correlation between reference hammer test and LSV tests

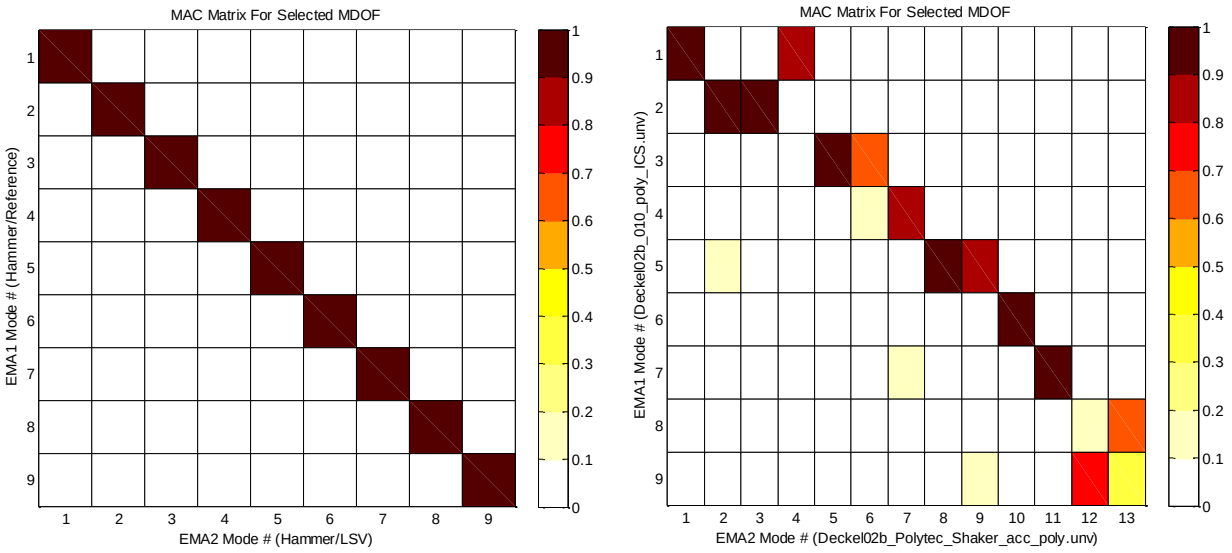

Figure 11: Test/test MAC matrices,
Hammer/Reference vs. Hammer/LSV (left) and Hammer/Reference vs. Shaker/LSV (right)

For test/analysis correlation the FE model with solid elements according to Figure 12 is employed.

The initial test/analysis correlation is shown in Table 4 and Figure 13 for the reference and LSV hammer tests and in Table 5 and Figure 14 for the LSV shaker test. As could already be expected from the findings above the correlation of the FE results to the hammer test results is more or less the same for both tests and shows a very good initial match of test and analysis.

For the LSV shaker test, however, larger deviations can be observed. Although all global modes of the cover can be paired, frequency deviations and MAC valued are compromised quite a bit due to the fact that the stinger is not (yet) included in the FE model.

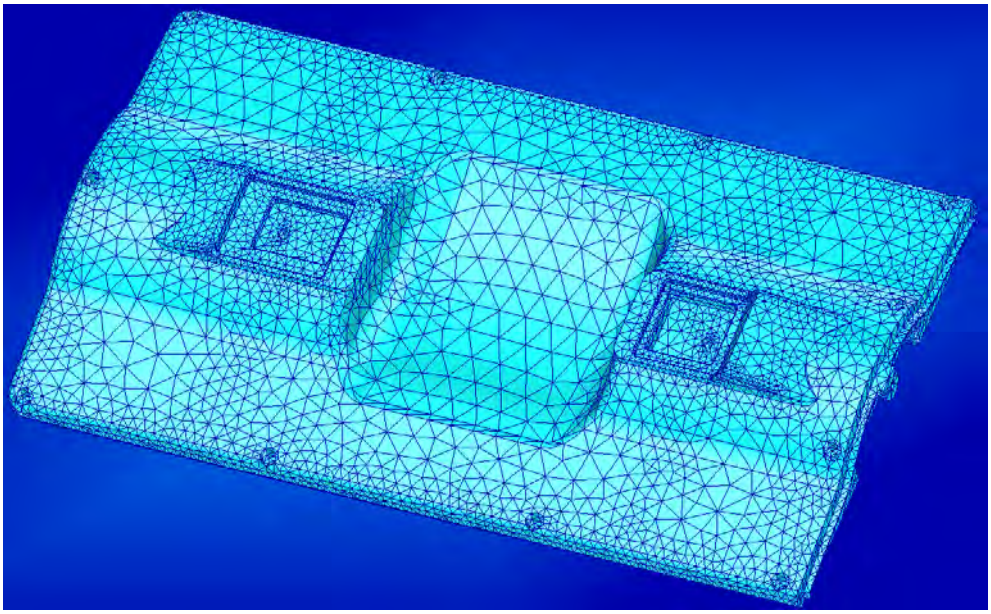

Figure 12: FE model of cover

No.	FEM [Hz]	Ref Ham. [Hz]	Dev. [%]	MAC [%]	LSV Ham. [Hz]	Dev. [%]	MAC [%]
1	458.44	453.78	1.03	99.90	452.15	1.39	99.92
2	573.60	568.42	0.91	99.67	567.26	1.12	99.92
3	1074.23	1081.34	-0.66	99.75	1079.79	-0.52	99.85
4	1374.01	1363.49	0.77	99.80	1360.72	0.98	99.82
5	1787.64	1769.39	1.03	99.74	1766.14	1.22	99.88
6	2355.10	2337.71	0.74	95.00	2332.96	0.95	96.80
7	2641.64	2644.03	-0.09	95.28	2639.55	0.08	96.99
8	2878.70	2867.14	0.40	97.20	2864.66	0.49	97.03
9	2969.79	2921.17	1.66	98.81	2914.78	1.89	98.91

Table 4: Test/analysis correlation for hammer tests

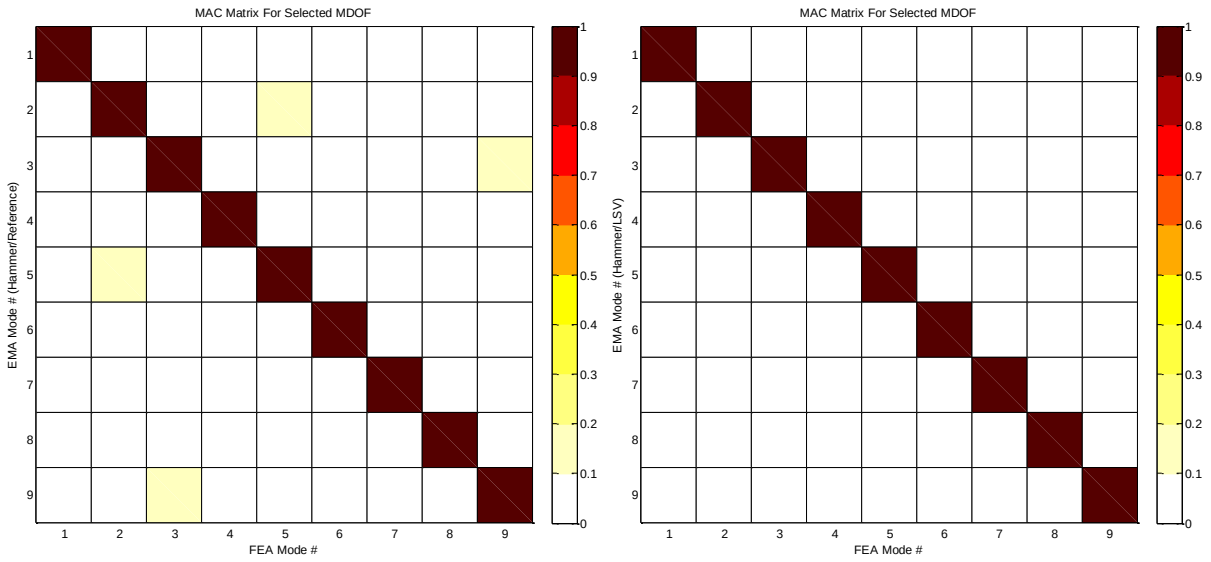

Figure 13: MAC matrices for hammer tests (left: Reference, right: LSV)

No.	FEM [Hz]	LSV Shak. [Hz]	Dev. [%]	MAC [%]
1	458.44	442.20	3.67	98.31
2	573.60	534.72	7.27	95.07
3	1074.23	989.08	8.61	87.14
4	1374.01	1336.76	2.79	91.62
5	1787.64	1822.47	-1.91	96.78
6	2355.10	2352.24	0.12	93.54
7	2641.64	2651.21	-0.36	89.19
8	2878.70	2893.87	2.62	83.08
9	2969.79	3031.78	-5.05	66.03

Table 5: Test/analysis correlation for LSV shaker test

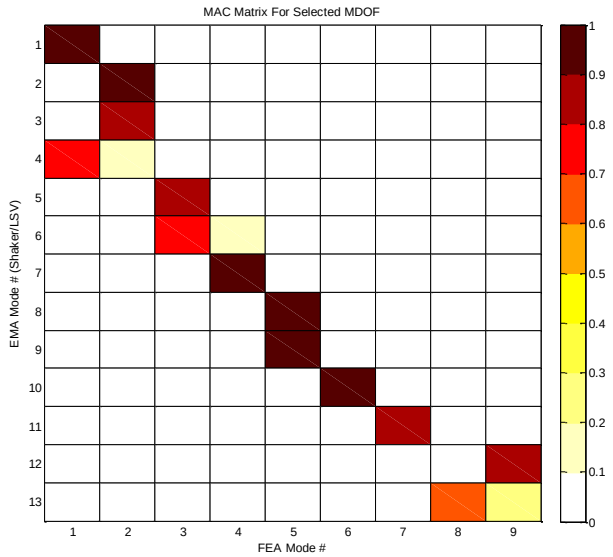

Figure 14: MAC matrix for LSV shaker test

5 Model validation

Based on the hammer test results, model validation can be restricted to simply adjusting the global Young's Modulus of the cover in order to reduce the mean value of the observed frequency deviations. However, since the correlation is already rather good this step may be neglected.

For the LSV shaker test results the impedance head/stinger assembly must be introduced to the model. Here it must be considered that the axial motion of the stinger is already decoupled from the system due to the force measurement. Figure 15 shows the additional impedance head/stinger assembly model which is based on the real geometry according to Figure 16.

Figure 15: FE model of impedance head/stinger assembly

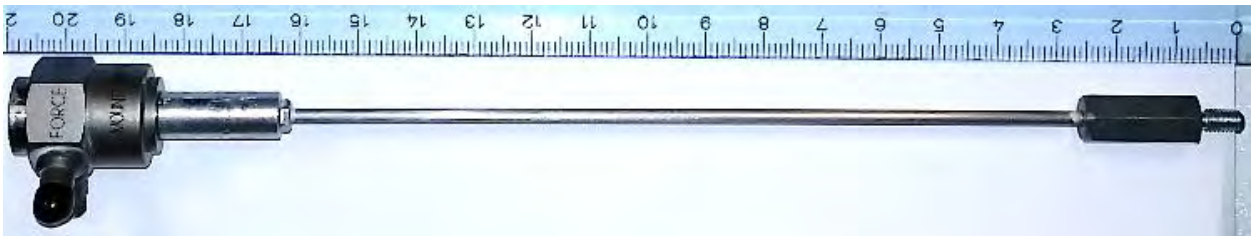

Figure 16: Impedance head/stinger geometry

Table 6 and Figure 17 now show the test/analysis correlation after implementation of the impedance head/stinger assembly. From Figure 17 it can be seen that if stinger and cover measurement degrees of freedom are considered, a relatively unique pairing of the modes can be obtained. However, test mode number seven (which is a global cover mode according to Tables 2 and 3) cannot be paired. The reason for this is the spatial misalignment of the local stinger modes between test and analysis with respect to the cyclic symmetry axis that – in this case – leads to a degradation of the MAC value.

If only the measurement degrees of freedom on the cover are considered mode seven is also paired, but the uniqueness of the pairing becomes significantly worse because of spatial aliasing of the cover modes when neglecting the additional measurement degrees of freedom on the stinger.

No.	FEM [Hz]	LSV Shak. [Hz]	Dev. [%]	MAC [%]
1	438.85	442.20	-0.76	99.23
2	527.70	534.72	-1.31	98.78
3	609.93	596.28	2.29	79.21
4	596.09	621.00	-4.01	97.82
5	973.77	989.08	-1.55	99.09
6	1171.47	1142.38	2.55	67.24
7	1441.99	1336.76	7.87	86.73
8	1730.12	1726.91	0.19	98.00
9	1930.49	1822.47	5.93	97.04
10	2367.40	2352.24	0.64	94.51
11	2638.26	2651.21	-0.49	92.71
12	2902.13	2893.87	0.29	75.94
13	3017.11	3031.78	-0.48	82.65

Table 6: Test/analysis correlation for LSV shaker test – model with impedance head/stinger assembly (only cover measurement degrees of freedom considered)

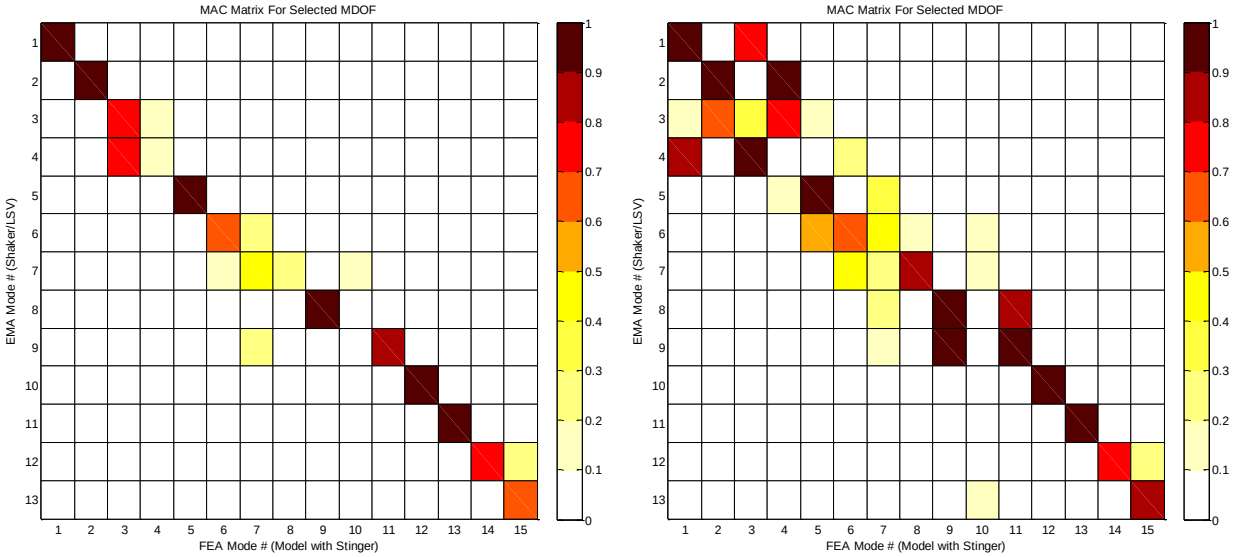

Figure 17: MAC matrix for LSV shaker test – model with impedance head/stinger assembly Stinger and cover (left)/only cover (right) measurement degrees of freedom considered

It can be noticed that all global modes can be paired again (marked in grey in Table 6) and up to 1 kHz the correlation is improved significantly. Above 1 kHz the situation is less clear. All in one the mean frequency deviation of the cover modes can be reduced by half from 2% to 1.1% and the mean MAC value is improved from 89% to 92%. Thus the systematic error for the LSV shaker test introduced by the impedance head/stinger assembly can be reduced substantially. However, in comparison to the hammer test correlations (see Table 4) the systematic errors cannot be fully removed. Main reason for this is, that parameter selection for the stinger model is rather difficult and itself prone to errors.

6 Summary and conclusions

In this paper, different excitation methods for experimental modal analysis were assessed by example of a lightweight aluminum cover in conjunction with classical acceleration measurements and laser scanning vibrometry.

It was shown that one of the greatest advantages of laser scanning vibrometry, namely the massless and practically interaction free automated response measurement with very high spatial resolution of lightweight structures can be compromised significantly if shaker excitation is employed. The effects observed included damping changes (presumably) due to micro friction between structure and impedance head, mass loading, and coupling of local stinger modes with global structural modes.

The first two effects may be minimized by selecting small and lightweight sensors, however, this is ultimately limited by physical boundaries. The latter effect may be minimized by selecting dedicated stinger geometries, e.g. bending-stiff stingers with local, highly flexible coupling in bending direction to shaker and impedance head. Yet these stingers are not always at hand and a complete removal of the systematic errors may not be achieved anyway.

While the influence of the stinger assembly is obvious, the potential influence of a roving hammer, as used for the reference test, on the test results is less apparent: the location and angle of the roving hammer impact position cannot be determined and/or controlled for every measurement point and thus introduces uncertainties. Moreover, the amount of uncertainty may also be related to the actual geometry of the tested structure and to subjective criteria as skill and experience of the hammer operator.

The influences of these uncertainties now depend upon the mode shape of the structure to be investigated. For lower modes with moderate curvature eventual deviations from the ideal impact position will have negligible influence; for higher modes, however, curvatures are usually much more complex and

deviations from the ideal impact position may introduce a significant error on amplitude and phase of the estimated mode shape component.

As an alternative to manual hammer excitation automated hammer measurements can be utilized. Next to the capability of fully automating the test sequence without the need for human interaction, automated hammers also bear the advantage of a very good reproducibility of the impact signal in direction, location, and force level. Since the force measurement is obtained at the hammer head itself, no force sensor needs to be attached to the structure to be measured. Thus, a practically interaction free automated measurement can also be achieved from the excitation side.

Especially in combination with roving laser scanning measurements, which as well provide a very accurate control of the sensing location (the laser focus typically has a diameter of less than 100µm), uncertainties as discussed above for the roving hammer test can be minimized which may be particularly beneficial for accurate measurements of higher order mode shapes.

All in one, promising results could be obtained applying the automated hammer technique in combination with laser scanning vibrometry and highly reliable data were measured. For the shaker excitation, systematic errors could not be entirely avoided and also an implementation of the impedance head/stinger assembly to the FE model could not fully account for these effects. Since an elimination of the effects was not possible using the shaker data may especially jeopardize the successful outcome of subsequent model validation campaigns.

References

[1] NV-Tech: *Scalable Automatic Hammer (SAM),* **http://nv-tech-design.de/**, Web product description